Electronic Supplementary Material (ESI) for Journal of Materials Chemistry B.

fNIR-responsive carbon-based nanocarriers for switchable on/off drug release and synergistic cancer therapy

Rongrong Nie,[a#] Hongji Liu,[b#] Lin Hu, [b] Xinyu Gu,[c] Junchao Qian,[d] and Hui Wang*[b]

a Nanjing Stomatological Hospital, Medical School of Nanjing University, Nanjing, 210008, Jiangsu, P. R. China

b The Anhui Key Laboratory of Condensed Matter Physics at Extreme Conditions, High Magnetic Field Laboratory, Hefei Institutes of Physical Science, Chinese Academy of Sciences, Hefei, 230031, Anhui, P. R. China.

c Department of Biochemistry, University of Washington, Seattle, 98195, Washington, United States

d Hefei Cancer Hospital, Hefei Institutes of Physical Science, Chinese Academy of Sciences, Hefei, 230031, Anhui, P. R. China

*Corresponding author: *E-mail: hw39@hmfl.ac.cn; Tel: +86-551-65590737*

# These authors contributed equally to this work

Experimental Section:

Materials: Doxorubicin (DOX) was purchased from Shanghai Sangon Biotech Company (Shanghai City, China). Ferrocene ($Fe(C_5H5)_2$, ≥98%), hydrogen peroxide (H_2O_2, 30%), acetone (C_3H_6O, 99%), ethanol (C_2H_6O, 99%), tetraethyl orthosilicate (TEOS, 98%), ammonia water ($NH_3 \cdot H_2O$, 27%), chitosan (low molecular weight), 1-ethyl-3-(3-dimethylaminopropyl) carbodiimide hydrochloride (EDC) were purchased from the Shanghai Chemical Factory. All chemicals were used as received without further purification.

Synthesis of silica NPs: Silica nanoparticles (NPs) were synthesized by the improved Stöber method.[1] Briefly, the mixed solution containing 75 mL ethanol and 6 mL ammonia water was vigorously stirred for 20 min at 60 °C. The TEOS (1.0 mL) was quickly added, and then the mixture was further stirred for 2 h, leading the formation of monodispersed silica NPs. The resultant products were purified with repeated centrifugation (12000 rpm, 10 min) and redispersion in water (50 mL) for three times. Finally, the silica NPs were dispersed in distilled water with a concentration of 4 mg/mL.

Synthesis of silica@magnetite@carbon NPs: In a typical synthesis, ferrocene (0.10 g) was dissolved in an acetone solvent (30 mL). After intense sonication for 5 min, 0.5 mL of silica NPs solution (4 mg/mL) were added into acetone solvent and the mixed solution was further sonicated for 20 min. 2.0 mL of hydrogen peroxide was slowly added into above mixed solution that was vigorously stirred for 20 min. Subsequently, the solution was transferred to a Teflon-lined stainless autoclave with a volume of 50.0 mL. The autoclave was maintained at 100 °C for 24 h and then heated to and maintained at 200 °C for 24 h. After cooling down to room temperature, the resultant silica@magnetite@carbon NPs was separated and then washed with acetone (30 mL) for three times. The as-prepared silica@magnetite@carbon NPs were collected for next use.

Synthesis of hollow magnetite@carbon dual-shell NPs: The as-prepared silica@magnetite@carbon NPs (0.5 g) were dispersed in 30 mL ammonia water. After being intensely sonicated for 30 min, the mixed solution was transferred to a Teflon-

lined stainless autoclave with a volume of 50.0 mL. The autoclave was heated to and maintained at 200 °C for 24 hours. After cooling down to room temperature, the resultant hollow magnetite@carbon dual-shell NPs was separated and then washed with distilled water (30 mL) for three times. Finally, the hollow magnetite@carbon dual-shell NPs were collected for next use.

Synthesis of CGC NCs: 5 mg EDC was added to 10 mL hollow magnetite@carbon dual-shell NPs solution (0.1 mg/ mL). The mixed solution was stirred for 1 h at room temperature. The chitosan solution (1 mL, 5 mg/mL) was quickly added into above solution with gentle stirring in darkness for 12 h. The resultant products were centrifuged (14 000 rpm, 30 min) and washed with PBS buffer (10 mL) for three times. Finally, the CGC NCs were collected for next characterization and applications.

Synthesis of DOX-loaded CGC NCs: The drug loading contains two steps. The one is to disperse hollow magnetite@carbon dual-shell NPs (1 mg) into DOX (2 mg)-dissolved PBS solution (10 mL, 0.005 M, pH = 7.4). After being stirred for 48 h at 37 ^{o} C, the mixture was separated and washed with PBS (10 mL) for three times by applying an external magnetic field. All the washed and separated solutions were collected. The amount of unloaded DOX molecules in the washed solution was quantified by a UV-Vis spectrophotometer at 480 nm. The drug loading content of the hollow magnetite@carbon dual-shell NPs was calculated by $[(M_0 - M_t)/M_N] \times 100\%$, where M_0 and M_t are the mass of DOX in the initial solution and washed solution, respectively. M_N is the mass of hollow magnetite@carbon dual-shell NPs used in the loading process.

The chitosan modification of DOX-loaded hollow magnetite@carbon dual-shell NPs was performed using above method (synthesis of CGC NCs). The released DOX during the modified process was collected and further quantified by a UV-Vis spectrophotometer at 480 nm. The drug loading content of the CGC NCs was calculated by comparing with the loaded drug of hollow magnetite@carbon dual-shell NPs and released DOX amount. Finally, the DOX-loaded CGC NCs were collected for next use.

Characterization: Transmission electron microscopy (TEM) images were taken on a transmission electron microscope (Hitachi H-7650) at an accelerating voltage of 100

kV. The elemental distributions were obtained using transmission electron microscopy (JEM-ARM200F). Powder X-ray diffraction (PXRD) patterns were performed on a Japan Rigaku D/MAX-cAX-ray diffractometer equipped with Cu Ka radiation. The UV-vis absorption spectra were obtained on a Thermo Electron Co. Helios β UV-vis Spectrometer. Raman spectrum was taken on a LABRAM-HR Confocal Laser Micro-Raman spectrometer using an Ar^+ laser with 514.5 nm at room temperature. The hydrodynamic size and surface charge were determined using Zetasizer Nano-ZS (Malvern Instruments, Worcestershire, UK) at the room temperature. Nitrogen adsorption–desorption measurements were carried out on a Micromeritics ASAP 2010 instrument to determine the BET surface area, single point total pore volume and BJH pore size distribution. The magnetic property was measured using a superconducting quantum interference device magnetometer (Quantum Design MPMS XL-7). In vitro and in vivo magnetic resonance (MR) imaging of CGC NCs were measured at 25 ℃ with a clinical MR scanner (GE HDxt, 3.0 T). Turbo Spin Echo (TSE) parameters: TR=5000 ms, effective TE=80 ms, echo train length (ETL) =15, FOV = 90 mm * 90 mm, matrix size = 180 * 180, slice thickness = 2.5 mm, 20 slices, number of averages = 2.

***In vitro* DOX release from DOX-loaded dual-shell NPs and DOX-loaded CGC NCs:** The *in vitro* release profiles of DOX from drug carriers were evaluated by the dialysis method. The DOX-loaded magnetite@carbon dual-shell NPs and DOX-loaded CGC NCs were dispersed in 5 mL PBS solution (0.005 M, pH = 7.4), respectively. Two dialysis bags filled with 2.5 mL DOX-loaded magnetite@carbon dual-shell NPs solution were immersed in 50 mL 0.005 M PBS solutions of pH = 7.4 at 37 ^{o}C subject or not subject NIR irradiation (808 nm, 1.5 W/cm^2) output power at certain releasing time intervals. Similarly, two dialysis bags filled with 2.5 mL DOX-loaded CGC NCs were immersed in 50 mL 0.005 M PBS solutions of pH = 7.4 at 37 ^{o}C subject or not subject NIR irradiation (808 nm, 1.5 W/cm^2) output power at certain releasing time intervals. The released DOX molecules outside the dialysis bags were sampled at defined time periods and assayed by UV-Vis spectrometry at 480 nm. Cumulative

release is expressed as the total percentage of drug released through the dialysis membrane over time.

Cell viability of CGC NCs or DOX-loaded CGC NCs with or without NIR irradiation: 4T1 cells were cultured in 96-well plates and incubated in 5% CO2 at 37 ºC for 24 h. Then different concentrations of DOX-loaded CGC NCs or CGC NCs (50, 25, and 12.5 μg/mL) were added. After that, the cells were further incubated for 72 h, and excess unbound materials were washed for three times with PBS. For photothermal treatments, the cells in the wells were irradiated with 1.5 W/cm^2 NIR light for 5 min. Subsequently, the relative cell viabilities (%) were detected by the alamar blue assay.

Histopathological evaluation of mice treated with CGC NCs or DOX-loaded CGC NCs: Five days after intravenous administration of DOX-loaded CGC NCs or CGC NCs (1 mg mL^{-1}, 200 μL per mouse), organs (heart, kidneys, liver, lungs and spleen) of BALB/c mice were collected by necropsy and fixed in 10% formalin for 48 h at 4°C. Tissues were then embedded in paraffin, sliced into 5 μm sections, and stained with hematoxylin and eosin. Microscopic images of tissues were acquired using a Nikon ECLIPSE TE2000-S microscope.

In vivo therapy with CGC NCs or DOX-loaded CGC NCs under NIR irradiation: All the animal procedures were in agreement with the guidelines for the care and use of laboratory animals of Ministry of Science and Technology of the People's Republic of China's requirements. The Animal Study Committee of Medical School of Nanjing University approved the experiments. Female BALB/c mice of 5 weeks old were used in this study. 4T1 cells were trypsinized, suspended in PBS and injected subcutaneously into the right flanks of these mice (1×10^6 cells per mouse). Mice were divided into six groups (n = 5 per group) and were administered intravenously every two days for a total of two times, with PBS, CGC or DOX-loaded CGC NCs (200 μL, 1 mg/mL). Twenty-four hours after every injection, certain groups of mice were subjected to NIR irradiation (808 nm, 1.5 W cm^{-2}) for 5 min. The length and width of tumors were measured by a caliper at different time points, and the tumor volume was calculated based on the following formula: $V = \text{width}^2 \times \text{length}/2$.

Supplemental Figures

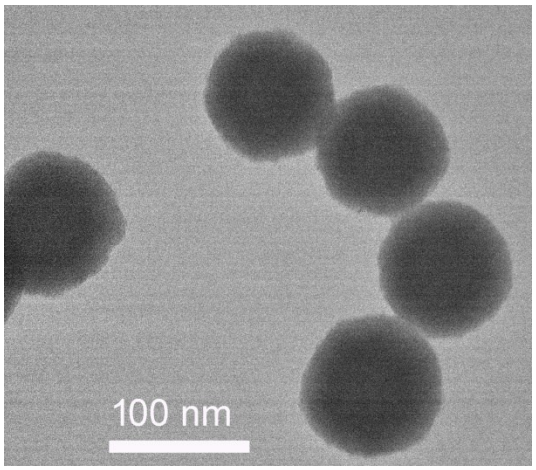

Fig. S1. TEM image of silica@magnetite@carbon core-shell-shell nanoparticles with an average size of 100 nm.

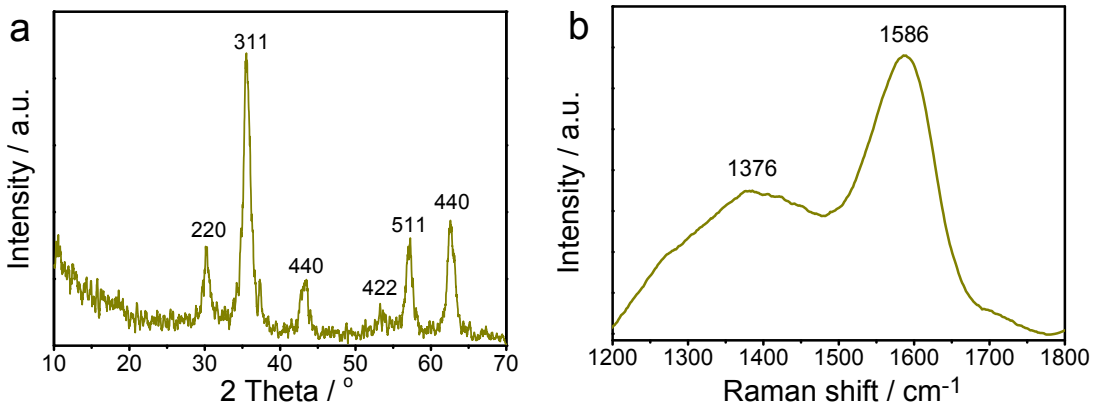

Fig. S2 (a) XRD patterns and (b) Raman spectrum of silica@magnetite@carbon core-shell-shell nanoparticles.

In the typical XRD pattern (Fig. S2a), the as-prepared nanoparticles show obviously reflections (220, 311, 400, 422, 511, 440), which can be indexed to the magnetite (Fe_3O_4) nanocrystals.[2] In typical Raman scattering patterns (Fig. S2b), the as-prepared nanoparticles show both peaks at 1586 cm^{-1} and 1376 cm^{-1}, which involves the G mode and D mode of the carbon shell, respectively.[3-5]

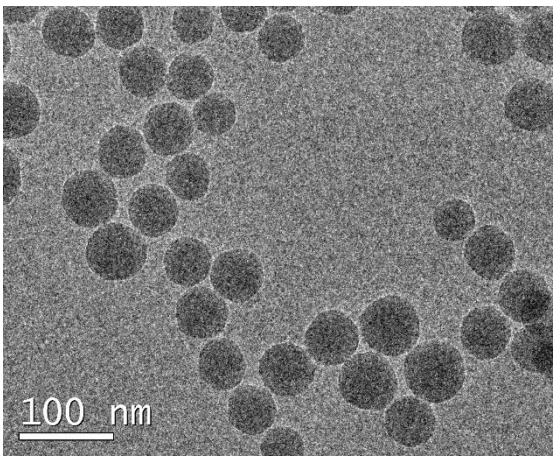

Fig. S3 TEM image of silica template nanoparticles with an average size of 55 nm.

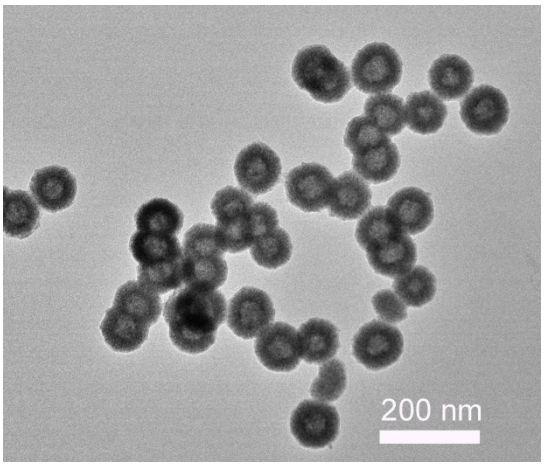

Fig. S4 TEM image of hollow magnetite@carbon nanoparticles with an average size of 100 nm.

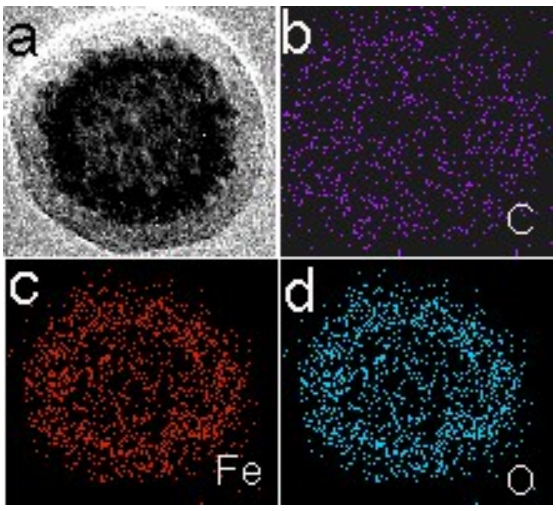

Fig. S5 (a) TEM image of single hollow magnetite@carbon nanoparticle; (b-d) distribution of different elemental in nanoparticle, (b) carbon; (c) iron and (d) oxygen.

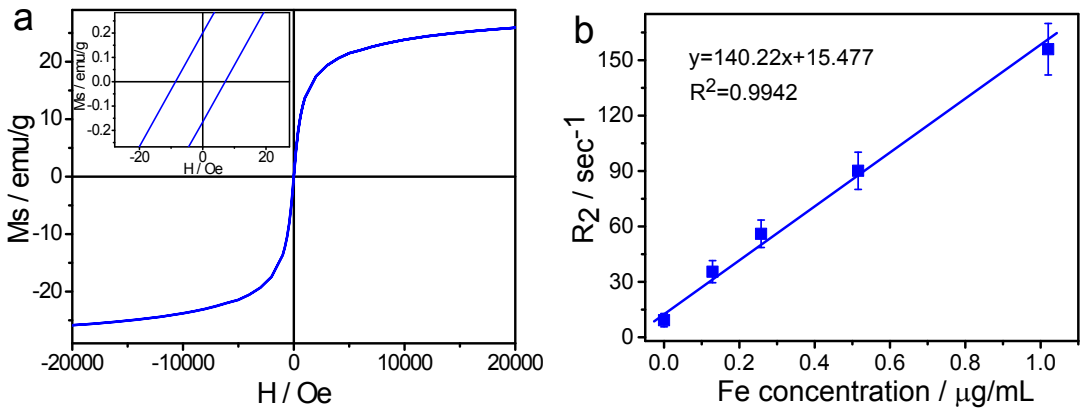

Fig. S6 (a) Hysteresis loop of CGC NCs measured at room temperature. The inset shows the respective expanded plots for fields between−4 and 4 Oe. (b) Relaxation of CGC NCs measured at 3.0 T. Plots of $1/T_2$ as a function of iron concentration. The slope of the curve in (b) is defined as the transverse relaxivity, r_2.

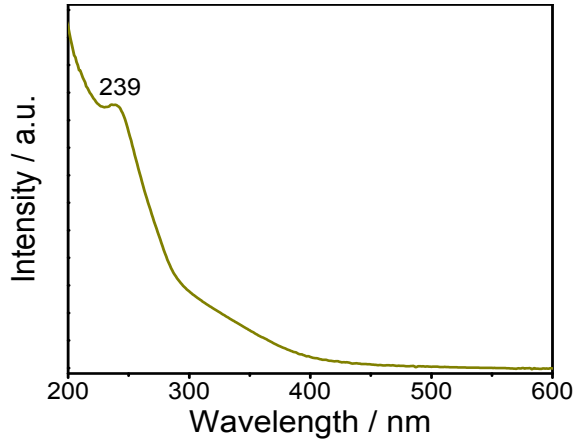

Fig. S7 UV-VIS absorption spectrum of hollow magnetite@carbon nanoparticles.

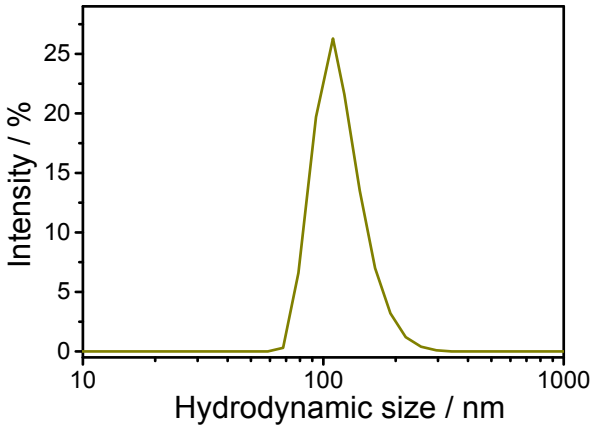

Fig. S8 Hydrophilic size distribution of hollow magnetite@carbon nanoparticles.

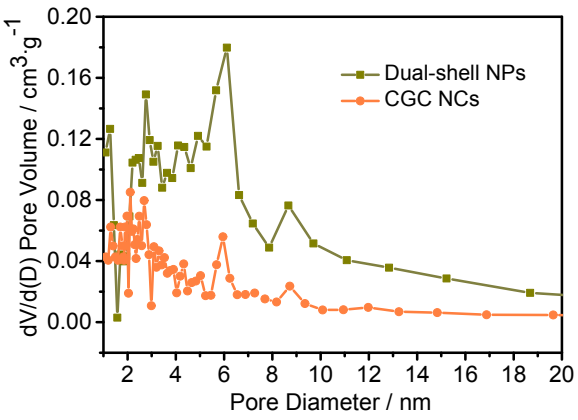

Fig. S9 Pore size distributions of magnetite@carbon dual-shell NPs and CGC NCs, respectively.

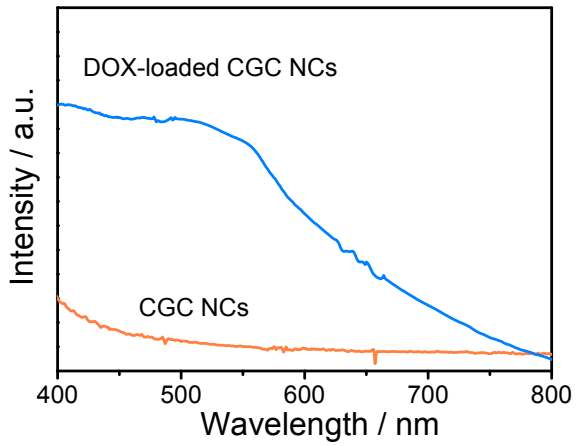

Fig. S10 VIS-NIR absorption spectra of CGC NCs and DOX-loaded CGC NCs, respectively.

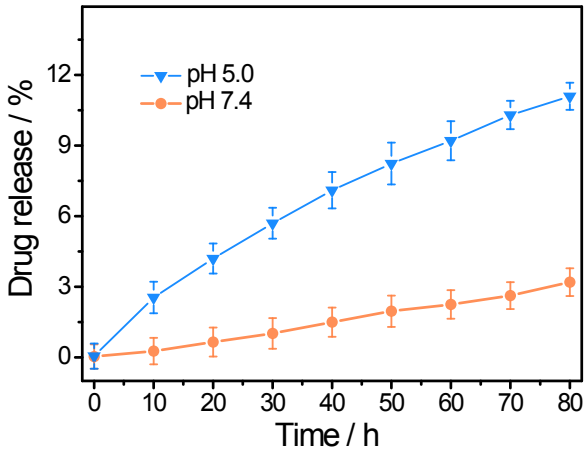

Fig. S11 Releasing profiles of DOX from CGC NCs in PBS with different pH at 37 °C.

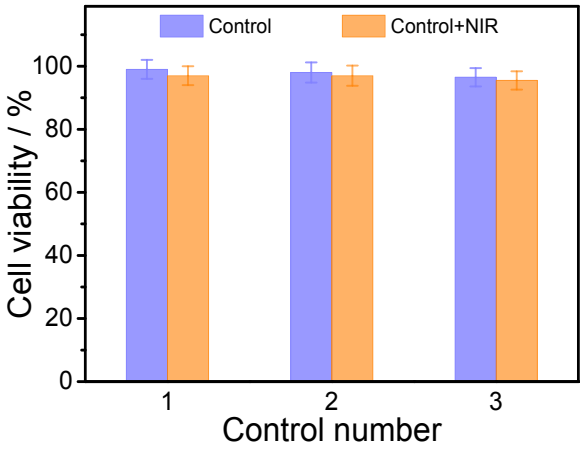

Fig. S12 Cell viability in the culture medium in the absence and presence of 1.5 W/cm^2 NIR for 5 min.

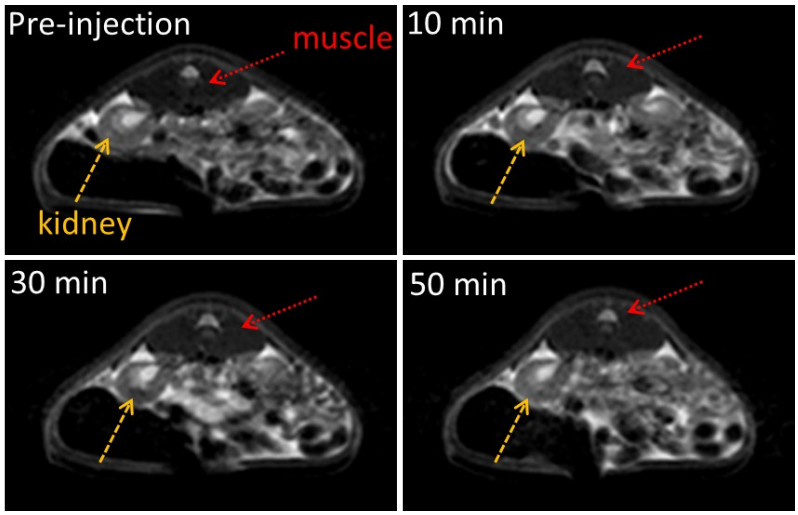

Fig. S13 In vivo T_2-weighted MR images of mice receiving CGC NCs through subcutaneous injection treatment (0.1 mg/mL, 200 μL) acquired before and after injections.

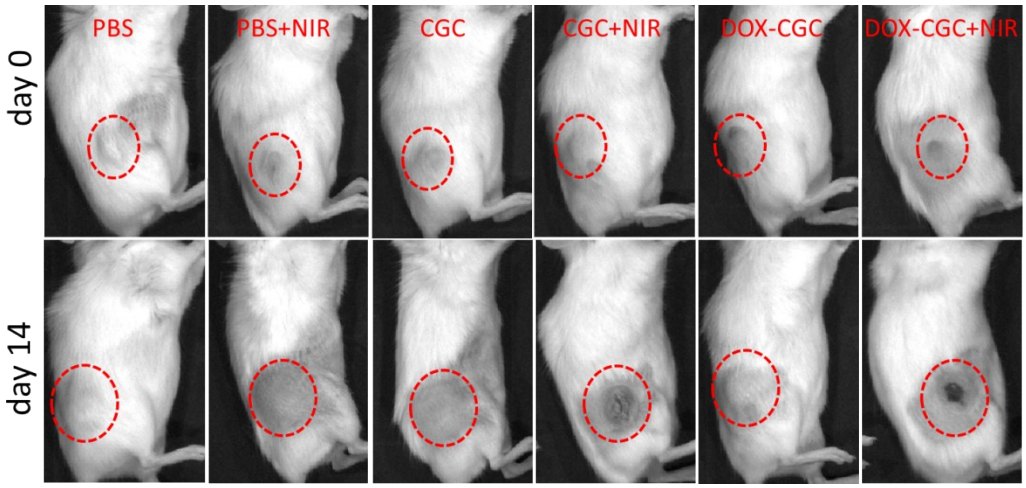

Fig. S14 Photographs of tumors in mice under various treatments at different treatments days (day 0 and day 14).

1. W. Stöber, A. Fink and E. Bohn, *Journal of Colloid and Interface Science*, 1968, **26**, 62-69.
2. H. Wang, Q.-W. Chen, Y.-F. Yu, K. Cheng and Y.-B. Sun, *The Journal of Physical Chemistry C*, 2011, **115**, 11427-11434.
3. A. C. Ferrari and J. Robertson, *Physical Review B*, 2000, **61**, 14095-14107.
4. J. Ristein, R. T. Stief, L. Ley and W. Beyer, *Journal of Applied Physics*, 1998, **84**, 3836-3847.
5. H. Wang, J. Zhuang, D. Velado, Z. Wei, H. Matsui and S. Zhou, *ACS Applied Materials & Interfaces*, 2015, **7**, 27703-27712.